Multivalley electron gas in a strong magnetic field

Zlatko Tešanović* and B. I. Halperin

Lyman Laboratory of Physics, Harvard University, Cambridge, Massachusetts 02138

(Received 14 April 1987)

We discuss the nonuniform high-field collective states of a multivalley electron gas. We consider specifically a model where there are two different orientations for the principal axes of the effective-mass tensor in the various valleys, and the magnetic field is applied along a direction that is symmetric with respect to these orientations. The onset of various instabilities is found within the Hartree-Fock approximation for the electron-hole correlations, as a function of the carrier density and magnetic field strength, the effective-mass anisotropy, the electronic g factor, and the number of degenerate valleys. Depending on the parameters, we find that the ground state may contain spin-density waves or valley-density waves—i.e., a state in which there are out-of-phase charge-density waves in various valleys. We discuss how the disorder that is present in most experimentally relevant systems may affect various collective transitions.

I. INTRODUCTION

Over the years there has been considerable interest in the properties of an interacting three-dimensional electron gas, in strong magnetic field, at low temperatures. In an early paper, Celli and Mermin[1] proposed that the ground state of this system should contain a spin-density wave with a wave vector oriented parallel to the magnetic field, provided that both spin states remain occupied. More recent discussions have concentrated on the strong field limit where all electron spins are parallel to the magnetic field; in this case the most prevalent finding is a ground state with charge-density waves of several different orientations, such as a Wigner crystal, or an array of charged rods, first considered by Kleppmann and Elliot.[2] Most of the analyses have been carried out using Hartree-Fock and related approximations or parquet equations.[3−6]

In the present paper, we extend this work to a situation where the electrons occur in two or more degenerate valleys. We consider the effects of effective-mass anisotropy in the valleys, and we consider the situation where the principal axes may have different orientations for different valleys.

Within our model we consider the possibility of several types of ground states, including spin-density wave (SDW) states and states we describe as valley-density wave (VDW) states. Depending on the parameters of the system, the SDW or VDW may have lower energy. The SDW we consider have separate spin-density waves for electrons in each valley. The wave vector of the SDW may have different directions in various valleys as a consequence of the different orientations of the effective-mass tensors in the valleys. In the simplest type of VDW state, there are separate charge-density wave states formed in each valley and each spin state. For each spin state the charge-density waves from two different valleys must lie in the same direction, and be 180° out of phase, in order that there be no inhomogeneity in the net charge density of the system, to lowest

order in the VDW amplitude. Because there are different densities of spin-up and spin-down electrons, their charge-density waves will have different wavelengths, and there cannot be cancelation of the CDW's between spin-up and spin-down electrons of the same or different valleys. We note that in a weak-coupling situation, where the gap due to the order parameter is small compared to the field-dependent Fermi energy, the energy cost of the first-order charge-density inhomogeneity is sufficiently great, that the system will generally avoid such a state. When the magnetic field becomes sufficiently strong, however, an inhomogeneous state, such as a Wigner crystal, may occur.

In addition to the type of VDW state described above, there are related VDW states in which electrons near the Fermi energy are placed in a linear combination of states from two different valleys. If the valley is indexed by an "isospin variable" $\tau=\pm 1$, this second type of VDW has an oscillating isospin polarization in the x-y plane, while the VDW described earlier is polarized in the z direction of isospin space. Within the approximations of our model, the two types of VDW states are exactly degenerate as long as the principal axes of all the valleys are identical. If this is not the case, however, the two polarizations of the VDW may have different energies. (We will discuss these questions further in Sec. IV and Appendix B.)

In general the VDW state will result in a modulation of the electron density and/or a modulation in the orbital magnetic moment at large wave vectors, comparable to the separation between valleys in the Brillouin zone. To lowest order in the VDW amplitude, however, there is no charge-density inhomogeneity at the smaller wave vectors which correspond to a wave vector difference between two points in the same electron valley. Thus, in weak coupling at least, we expect the VDW states to have lower energy than a simple CDW state.

Our calculations are carried out in the Fukuyama approximation to the Hartree-Fock equations,[7] in which the nonlocal exchange potential is replaced by an aver-

age over momentum components parallel to the magnetic field. In general, we do not actually solve the problem of the ground-state energy, but rather look for the transition temperature at which the uniform electron gas becomes unstable to a broken symmetry of the various types considered. At least in the weak-coupling limit, the form of the ground state can be inferred from this analysis.

It should be mentioned that the present model cannot be applied directly to actual semiconductors or semimetals. In doped semiconductors, the random potential of impurities is a big perturbation, which may have a drastic effect on the ground state. In the weak-coupling regime, where the electron-electron interaction is small compared to the kinetic energy, the impurity potential will destroy the predicted phase transition, and eliminate the ordering completely. In the strong-coupling regime, however, near the metal-insulator transition at zero magnetic field, it is possible that local ordering persists, and perhaps even a phase transition under certain circumstances. Although a Hartree-Fock calculation cannot be trusted in this regime, the analysis of the present paper may still be useful in suggesting the types of states that could occur.

Our analysis may be more applicable to a semimetal, such as graphite, where a phase transition has already been observed in strong magnetic fields.[8] A proper analysis of the semimetal case must allow for two kinds of carriers, electrons and holes, in different parts of the Brillouin zone, or a nonparabolic band structure, if the electrons and holes are in the adjacent regions of the zone. Also, at high carrier densities, one must take into account electron-electron scattering between different valleys, which has not been included in our model. The "charge-density wave" state proposed by Yoshioka and Fukuyama[4] for the case of graphite in a strong magnetic field is actually a VDW state, in our notation, since there are CDW's for two different valleys which are 180° out of phase.

II. DESCRIPTION OF THE MODEL

We assume that the effective-mass tensor in each electron valley has axial symmetry, with a doubly degenerate transverse eigenvalue m_t, and a single longitudinal eigenvalue m_l (we assume $m_t < m_l$). The important dimensionless parameters which characterize the band structure of the system are then the number of degenerate valleys N_v, the mass anisotropy ratio m_t/m_l, and the angles between the longitudinal axes of the various valleys.

In the presence of an applied magnetic field there are additional dimensionless parameters which describe the orientation of field relative to the symmetry axes of the valleys. Another important dimensionless parameter is given by $g^* = m_t g$, where m_t is given in units of the bare electron mass, and $g/2$ is the spin magnetic moment of the carriers, in units of the free electron Bohr magneton (for simplicity we assume that the g factor is isotropic; more generally the g factor should be represented by a tensor with longitudinal and transverse components in each valley). If the magnetic field is applied along the

symmetry axis of some valley, then the ratio of the Zeeman energy to the cyclotron energy is equal to $g^*/2$ for carriers in that valley.

It should be remarked the dimensionless material parameters defined above vary considerably from one material to another, and they may differ greatly from the free electron values. For example, in n-type Ge there are four electron valleys, the mass ratio m_t/m_l is ≈ 0.05, and the parameter g^* is also of order 0.05.

When a finite density of carriers is present in the system, two more dimensionless parameters come into play: One parameter is the ratio of the Fermi energy to an energy, such as Zeeman energy, which measures the strength of the magnetic field; the second is a quantity r_s which measures the relative importance of the electron-electron interaction and the kinetic energy of the system. In doped semiconductors these are experimental parameters which can be varied by altering the doping concentration and the external magnetic field. In a semimetal the carrier concentration is determined by the band structure of the material, but some variation may still be obtained by application of pressure or by adding impurities to the material.

It is clearly not practical to explore all regions of parameter space for a model where the number of important parameters is large. However, we can hope to gain some insight by looking at some illustrative examples, where a representative value is chosen for each of the various parameters, except for the field strength which we vary continuously in an interesting range. One case which is easy to discuss is the isotropic situation, where $m_t = m_l$. Also relatively simple is the case when all occupied electron valleys are oriented in the same direction. In order to illustrate the situation for valleys of different orientations, we shall choose a model where there are valleys of two different orientations, and an equal number of valleys $N_v/2$ for each orientation. The magnetic field in this case will be taken along a direction which bisects the angle between the axes of the two valleys.

To define the model further, we shall take the z direction to be the direction of the applied magnetic field $\mathbf{B}$. The symmetry axis of each occupied valley α $(\alpha = 1, \ldots, N_v)$ is assumed to lie in the y-z plane at an angle θ_α with z direction. For the case of two different valley orientations, this means that there are two classes of valleys, "left valleys" and "right valleys," for which θ_α is chosen to be, respectively, $-\theta$ and θ, where 2θ is the angle between the two valley axes. This situation is shown in Fig. 1.

We choose to work in the Landau gauge with vector potential $\mathbf{A} = (-By, 0, 0)$. Then the one-electron eigenstates for an electron in valley α are described, in the effective mass approximation, by the envelope function

$$\Psi_{n k_x k_z \alpha}(\mathbf{r}) = \frac{1}{L} \exp \left[i k_z z + i k_x x - i \frac{b_\alpha}{a_\alpha} k_z (y + l^2 k_x) \right]$$

$$\times \Phi_{n\alpha}(y + l^2 k_x) ,$$

where $\alpha = 1, \ldots, 2N_v$ is a valley index,

$$a_\alpha \equiv \frac{\cos^2\theta_\alpha}{m_t} + \frac{\sin^2\theta_\alpha}{m_l} \ ,$$

$$b_\alpha \equiv \cos\theta_\alpha \sin\theta_\alpha \left[\frac{1}{m_t} - \frac{1}{m_l} \right] \ ,$$

$l = \sqrt{(c/eB)}$, and

$$\Phi_{n\alpha}(y) = \frac{1}{(2^n n! \sqrt{\pi}l_\alpha)^{1/2}} H_n \left[\frac{y}{l_\alpha} \right] \exp \left[-\frac{1}{2}\frac{y^2}{l_\alpha^2} \right] \ ,$$

with H_n being Hermite polynomials,

$$l_\alpha = l \left[\cos^2\theta_\alpha + \frac{m_t}{m_l}\sin^2\theta_\alpha \right]^{1/4} \ ,$$

and L is the linear size of the system. The energy corresponding to this state is

$$E_{nk_z\alpha} = (n + \tfrac{1}{2})\omega_{c_\alpha} + \frac{k_z^2}{2m_\alpha} \ ,$$

with

$$m_\alpha \equiv \left[\frac{\sin^2\theta_\alpha}{m_t} + \frac{\cos^2\theta_\alpha}{m_l} - \frac{b_\alpha^2}{a_\alpha} \right]^{-1} \ ,$$

and

$$\omega_{c_\alpha} \equiv \frac{eB}{c} \left[\frac{a_\alpha}{m_t} \right]^{1/2} \ .$$

(For derivation of the above single-particle eigenfunctions and energy eigenvalues, see Appendix A.) From now on we restrict ourselves to the case when only the lowest Landau level is occupied, i.e., $n = 0$.

Within our model, the Hamiltonian for the electron gas in a magnetic field can be written as follows:

$$H = \sum_{k_x, k_z} \sum_{s, \alpha} \xi_{k_z, \alpha} c^\dagger_{k_x k_z s\alpha} c_{k_x k_z s\alpha} + g\mu_B S_z B$$

$$+ \tfrac{1}{2} \sum_q V(q) \sum_{\alpha, \beta} \left[\rho_\alpha(q)\rho_\beta(-q) - \exp\left[-\frac{l_\alpha^2 q_\perp^2}{2} \right] \rho_\alpha(0)\delta_{\alpha\beta} \right] \ , \tag{2.1}$$

where $\xi_{k_z\alpha} \equiv E_{k_z\alpha} - \mu$, s is a spin index, μ_B is the Bohr magneton, $\rho_\alpha(q)$ is density operator for electrons in valley α, restricted to the lowest Landau level (explicit form for the density operator is given in Appendix B), $q_\perp \equiv (q_x, q_y)$, and we are considering the long-range form of the Coulomb potential $V(q) = (4\pi e^2/\epsilon_0 L^3 q^2)$, L^3 being the total volume of the system. We have assumed here that the quantum limit has been attained in which only the lowest Landau level with *both* spin levels is occupied, implying

$$g < 2 \left[\frac{\cos^2\theta_\alpha}{m_t^2} + \frac{\sin^2\theta_\alpha}{m_t m_l} \right]^{1/2} \ ,$$
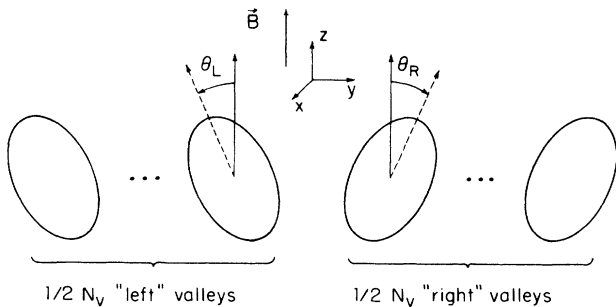

FIG. 1. The model of the multivalley Fermi surface. All valleys are identical except for the orientation of the principal axis, which is directed either at the angle $\theta = \theta_R$ or $-\theta = \theta_L$ with respect to the magnetic field **B**. There are $\tfrac{1}{2}N_v$ "left" and $\tfrac{1}{2}N_v$ "right" valleys.

where m_t and m_l are given in units of the bare electron mass m_e. In practice this can be accomplished with moderately strong fields in several degenerate semiconductors.[9] The case with several Landau levels occupied can be treated along similar lines. We also ignore the intervalley scattering which is very small and can be neglected to a good approximation in most semiconductors.[10]

In the quantum limit the spectrum of single particle excitations appears effectively one dimensional, leading to an anomalous increase in the response functions at the wave vector $q_z = k^F_{\alpha s_1} + k^F_{\beta s_2}$, where $k^F_{\alpha s}$ is the Fermi momentum in the direction of the field for valley α and the spin state s. This makes the system susceptible to various instabilities. In this paper we calculate the response functions in the uniform system, within the Hartree-Fock approximation for the mutual Coulomb interaction, and look for the temperature where the appropriate response function diverges.

In the noninteracting electron gas, the response function is proportional to the particle-hole bubble, i.e., the Lindhard function. In the quantum limit, the particle-hole excitation spectrum is quasi-one-dimensional, and the Lindhard function $D_{\alpha\beta, s_1 s_2}(\mathbf{q}, \omega)$ depends only on the z component of the wave vector $\mathbf{q}$; indices α and s_1 refer to the particle propagator while β and s_2 correspond to the hole. For our purposes only the static (i.e., $\omega = 0$) Lindhard function is needed which is given by

$$D_{\alpha\beta, s_1 s_2}(q_z) = \frac{L^3}{(2\pi l)^2} \int \frac{dk_z}{2\pi} \frac{f(\xi_{k_z, \alpha s_1}) - f(\xi_{k_z + q_z, \beta s_2})}{\xi_{k_z, \alpha s_1} - \xi_{k_z + q_z, \beta s_2}} \ ,$$

where f is the Fermi function. $D_{\alpha\beta,s_1s_2}(q_z)$ exhibits a well-known "one-dimensional" logarithmic singularity at $T=0$ when $q_z=k_{F_{s_1}}^{\alpha}+k_{F_{s_2}}^{\beta}$; if we consider the finite temperature case, this singularity is cut off by T. We will be typically interested in the value of the Lindhard function at the wave vectors where the zero temperature singularity occurs. In the weak-coupling regime, the transition temperature T_c, at which the response of an *interacting* system diverges, satisfies $T_c \ll E_{\alpha s}^F$ for each α and s, where $E_{\alpha s}^F=(k_{\alpha s}^F)^2/2m_\alpha$ is the Fermi energy in a given valley and spin state. Then the Lindhard function

$$D_{\alpha\beta,s_1s_2}(q_z=k_{\alpha s_1}^F+k_{\beta s_2}^F)$$

has the following form:

$$D_{\alpha\beta,s_1s_2}=-\frac{2L^3(m_\alpha m_\beta)^{1/2}}{(2\pi l)^2(k_{\alpha s_1}^F+k_{\beta s_2}^F)}$$
$$\times\ln\left|1.14\frac{k_{\alpha s_1}^F k_{\beta s_2}^F}{2(m_\alpha m_\beta)^{1/2}T_c}\right|.$$

In searching for the various instabilities we are interested in the spin, valley, and charge-density responses of the interacting system. The general form for these response functions can be written as[11]

$$\chi_A(\mathbf{q},\omega)=-i\int_0^\infty dt\, e^{i\omega t}\langle[A(\mathbf{q},t),A^\dagger(\mathbf{q},0)]\rangle\,,\qquad(2.2)$$

where $\langle\ \rangle$ denotes quantum mechanical and thermal averaging and $A(\mathbf{q},t)$ refers to the single-particle operators like the particle-density operator $\rho(\mathbf{q},t)$, the spin-density operators $\sigma(\mathbf{q},t)$, and the "valley-density" operators $\tau(\mathbf{q},t)$. The explicit forms for these operators are given in Appendix B.

In the noninteracting case, the response function is given by

$$\chi^A(\mathbf{q},\omega)=\sum_{\alpha,\beta}M_{\alpha\beta,s_1s_2}^A(\mathbf{q})D_{\alpha\beta,s_1s_2}(\mathbf{q},\omega)$$
$$\times M_{\alpha\beta,s_1s_2}^{A*}(\mathbf{q})\,,\qquad(2.3)$$

where $M_{\alpha\beta}^A(\mathbf{q})$ contains the matrix elements of various density operators

$$M_{\alpha\beta,s_1s_2}^A(\mathbf{q})=\exp\left[-\frac{l^4}{4l_{\alpha\beta}^2}q_x^2-\frac{l_{\alpha\beta}^2}{4}q_y^2-\frac{l_{\alpha\beta}^2}{16}\left[\frac{b_\alpha}{a_\alpha}+\frac{b_\beta}{a_\beta}\right]^2q_z^2+\frac{l_{\alpha\beta}^2}{4}\left[\frac{b_\alpha}{a_\alpha}+\frac{b_\beta}{a_\beta}\right]q_zq_y\right]\langle\alpha s_1|\Theta_A|\beta s_2\rangle\,,$$

with $l_{\alpha\beta}^{-2}\equiv\frac{1}{2}(l_\alpha^{-2}+l_\beta^{-2})$. The matrix elements $\langle\alpha s_1|\Theta_A|\beta s_2\rangle$ are given explicitly in Appendix B. In the interacting system, it is convenient to work with the function $P_{\alpha\beta,s_1s_2}^A(\mathbf{q},\omega)$, which is defined by

$$\chi^A(\mathbf{q},\omega)=\sum_{\alpha,\beta}M_{\alpha\beta,s_1s_2}^A(\mathbf{q})P_{\alpha\beta,s_1s_2}^A(\mathbf{q},\omega)\,.\qquad(2.4)$$

To find the temperature and wave vectors at which $P_{\alpha\beta,s_1s_2}^A(\mathbf{q})$ diverges (we now consider only the static response), we need an explicit form for the interacting response function. Here we use the Hartree-Fock approximation to determine $P_{\alpha\beta,s_1s_2}^A(\mathbf{q})$. This approximation consists of summing the electron-hole bubbles for a direct interaction and the self-consistent vertex correction for an exchange part.[7] The diagrams included in the Hartree-Fock approximation are depicted in Fig. 2(a). The bare interaction $V(\mathbf{q})$ defined earlier is scaled down by familiar Gaussian factors; we define

$$\tilde{V}_{\alpha\beta}(\mathbf{q})=V(\mathbf{q})\exp\left[-\left[\frac{l^4}{4l_\alpha^2}+\frac{l^4}{4l_\beta^2}\right]q_x^2-\left[\frac{l_\alpha^2}{4}+\frac{l_\beta^2}{4}\right]q_y^2\right].$$

Furthermore, as a direct consequence of anisotropy, there are additional $f_\alpha(k_x,k_z,\mathbf{q})$ factors that contribute to the bare electron-electron vertex as shown in Fig. 2(b). They are given by

$$f_\alpha(k_x,k_z,\mathbf{q})=\exp\left[-i\frac{b_\alpha}{a_\alpha}l^2k_zq_x+\frac{l_\alpha^2b_\alpha}{2a_\alpha}q_yq_z-\frac{l_\alpha^2b_\alpha^2}{4a_\alpha^2}q_z^2\right].$$

These factors can be included in the definition of the electron-hole correlation functions without affecting their pole structure. (The above expressions for $\tilde{V}$ and f_α are derived in Appendix C. There is some arbitrariness associated with this particular factorization. We have chosen to define $\tilde{V}$ in a way that naturally extends the notation of Ref. 7.)

Summation of Hartree-Fock diagrams leads to a complicated integral equation for the response function which is difficult to treat exactly. Here we can use the fact that we are working in the strong field limit ($k_Fl\ll1$) and use Fukuyama's approximation[7] for the exchange integral. In this approximation one replaces the exchange part by its average over the relevant momentum range in the z direction (this range extends typically from $k_{\alpha s_1}^F$ to $k_{\beta s_2}^F$). In this way we obtain

$$P_{\alpha\beta,s_1s_2}^A(\mathbf{q})=M_{\alpha\beta,s_1s_2}^{*A}(\mathbf{q})D_{\alpha\beta,s_1s_2}^f(q_z)+\delta_{\alpha\beta}\delta_{s_1s_2}D_{\alpha\beta,s_1s_2}^f(q_z)\tilde{V}(\mathbf{q})\mathrm{Tr}P^A(\mathbf{q})-D_{\alpha\beta,s_1s_2}(q_z)W_{\alpha\beta,s_1s_2}(\mathbf{q})P_{\alpha\beta,s_1s_2}^A(\mathbf{q})\,.\qquad(2.5)$$

In (2.5) $D_{\alpha\beta,s_1s_2}^f$ is defined as $f_\alpha(\mathbf{q})f_\beta(\mathbf{q})D_{\alpha\beta,s_1s_2}$. In the Fukuyama approximation, the exchange interaction W is

given by

$$W_{RR,s_1 s_2}(\mathbf{q}) = \sum_{p\perp} \int_{-k_{s_1}^F}^{k_{s_2}^F} \frac{dp}{2(k_{s_1}^F + k_{s_2}^F)} \exp\left[-\frac{l^4}{2l_R^2}p_x^2 - \frac{l_R^2}{2}p_y^2 - \frac{l_R^2 b_R^2}{2a_R^2}p^2 \right] \frac{4\pi e^2}{\epsilon_0 L^3} \frac{1}{p_\perp^2 + p^2} \cos\left[l^2 \left(q_y - \frac{b_R}{a_R}q_z \right)p_x \right]$$

$$\times \left[\cos(l^2 p_y q_x)\cosh\left[l_R^2 \frac{b_R}{a_R}p_y p \right]\cos\left[l^2 \frac{b_R}{a_R}q_x p \right] \right.$$

$$\left. - \sin(l^2 p_y q_x)\sinh\left[l_R^2 \frac{b_R}{a_R}p_y p \right]\sin\left[l^2 \frac{b_R}{a_R}q_x p \right] \right] + (s_1 \rightarrow s_2), \tag{2.6}$$

$$W_{RL,s_1 = s_2}(\mathbf{q}) = \sum_{p\perp} \frac{\sin[2(b_R/a_R)l^2 k_{s_1}^F p_x]}{2(b_R/a_R)l^2 k_{s_1}^F p_x} \int_{-k_{s_1}^F}^{k_{s_1}^F} \frac{dp}{2k_{s_1}^F}\exp\left[-\frac{l^4}{2l_R^2}p_x^2 - \frac{l_R^2}{2}p_y^2 - \frac{l_R^2 b_R^2}{2a_R^2}p^2 \right]$$

$$\times \frac{4\pi e^2}{\epsilon_0 L^3} \frac{1}{p_\perp^2 + p^2}\cos(l^2 p_y q_x)\cos(l^2 p_x q_y). \tag{2.7}$$

Subscripts L and R denote valleys at angles $-\theta$ and θ with respect to $\mathbf{B}$, respectively, while $\theta_L = -\theta$ and $\theta_R = \theta$ in accordance with Fig. 1. $W_{LL,s_1 s_2}$ and $W_{LR,s_1 = s_2}$ are found from (2.6) and (2.7) by replacing θ_R with θ_L, while $W_{LR,s_1 \neq s_2}$ is not needed for our purposes. In (2.7) we specified $\theta_L = -\theta_R$; if this is not the case, the expression for W_{RL} and W_{LR} is quite a bit more complicated. This is a closed system of equations for the response functions.

In the following two sections, we calculate the transition temperatures for SDW and VDW states for various values of parameters of our model, discussing separately isotropic and anisotropic cases. Transition temperatures will be evaluated as functions of the magnetic field which is allowed to vary in the interval from B_1, the field above which only the lowest Landau level with both spin states is occupied to B_2, where the spin-down band is completely empty. For the general anisotropic case, when $\theta \neq 0$ and $m_t \neq m_l$, these two limiting fields are given by the following expressions:

$$B_1^3 = \frac{B_0^3}{d_\alpha}\frac{8}{\tilde{g}^2}[1 - \tfrac{1}{2}\tilde{g} - (1-\tilde{g})^{1/2}] \tag{2.8}$$

and

$$B_2^3 = 4\frac{B_0^3}{d_\alpha \tilde{g}}, \tag{2.9}$$

where $B_0^3 = \pi\Phi_0^3 n^2/16N_v^2$, Φ_0 being the elementary flux quantum and n the total density of the system, $d_\alpha \equiv m_\alpha a_\alpha^{1/2}/m_t^{1/2}$ and

$$\tilde{g} = \frac{m_\alpha}{d_\alpha}g. \tag{2.10}$$

III. ISOTROPIC CASE

To see a qualitative effect of the valley degeneracy, let us further simplify (2.5) by assuming $m_t = m_l$.[12] In this case we have N_v identical valleys and Hamiltonian (2.1)

possesses a full $SU(N_v)$ valley symmetry (we therefore drop the valley index throughout this section). If we now consider solutions of (2.5) we immediately see that, for large N_v, the charge density response $P^{CDW}(\mathbf{q})$ does not have a singularity at all. In this case Θ_A is a unit matrix, and the positive second term on the right-hand side of (2.5) (i.e., the "direct term") is enhanced by $\mathrm{Tr}P^{CDW} \propto N_v$. Actually, for isotropic valleys the CDW is never a favored state in the Hartree-Fock approximation. This is easy to see: In the absence of valley degeneracy, SDW can take advantage of the exchange energy without coupling to the direct part, but it is eventually destabilized by the Zeeman energy, which causes depopulation of the up-spin band. For valleys, there is no Zeeman energy; therefore, the VDW can always take the full advantage of the exchange part resulting in the transition temperature higher than that of CDW. It is, however, interesting to consider the relative stability of SDW and VDW states.

In the weak-coupling limit that we are considering, the temperature at which P^A diverges has the following generic form:

$$T_c^A(\mathbf{q}_\perp) = 1.14 E_A^F e^{-1/\lambda_A(\mathbf{q}_\perp)}, \tag{3.1}$$

where we have set $q_z = k_{s_1}^F + k_{s_2}^F$ since we expect that, in the weak-coupling regime, this value of q_z corresponds to highest T_c by virtue of the logarithmic singularity in $D_{\alpha\beta,s_1 s_2}(q_z)$. For spin-density waves which are formed independently in each valley, the "cutoff" E_A^F is provided by $E_{\uparrow\downarrow}^F = (k_\uparrow^F k_\downarrow^F/2m)$ (Here $\uparrow$ and $\downarrow$ stand for the $+1$ and -1 eigenvalues of the spin angular momentum operator σ_z. They denote the up- and down-spin bands, respectively). The coupling constant λ_A is given in this case as

$$\lambda^{SDW}(\mathbf{q}_\perp) = \frac{2L^3 m}{(2\pi l)^2(k_\uparrow^F + k_\downarrow^F)}W^{SDW},$$

$$\mathbf{q}_\perp, q_z = k_\uparrow^F + k_\downarrow^F, \tag{3.2}$$

where

$$W^{SDW}(q_\perp, q_z = k_\uparrow^F + k_\downarrow^F) = \frac{4\pi e^2 l^2}{\epsilon_0 L^3} \int_0^\infty dx\, e^{-x^2/2} \frac{J_0(lxq_\perp)}{\rho_\uparrow + \rho_\downarrow} \left[\arctan\frac{\rho_\uparrow}{x} + \arctan\frac{\rho_\downarrow}{x} \right] ,$$

$J_0(lxq_\perp)$ being the Bessel function and $\rho_{\uparrow(\downarrow)} \equiv lk_{\uparrow(\downarrow)}^F$. The variable of integration is $x \equiv lp_\perp$. Similarly, for valley-density waves which are formed as out-of-phase charge density waves in left and right valleys E_A^F is given by $E_{\uparrow(\downarrow)}^F = (k_{\uparrow(\downarrow)}^F)^2/2m$ for the up(down)-spin band and

$$\lambda^{VDW\uparrow(\downarrow)}(q_\perp) = \frac{L^3 m}{(2\pi l)^2 k_{\uparrow(\downarrow)}^F} W^{VDW\uparrow(\downarrow)}, \quad q_\perp, q_z = 2k_{\uparrow(\downarrow)}^F ,$$
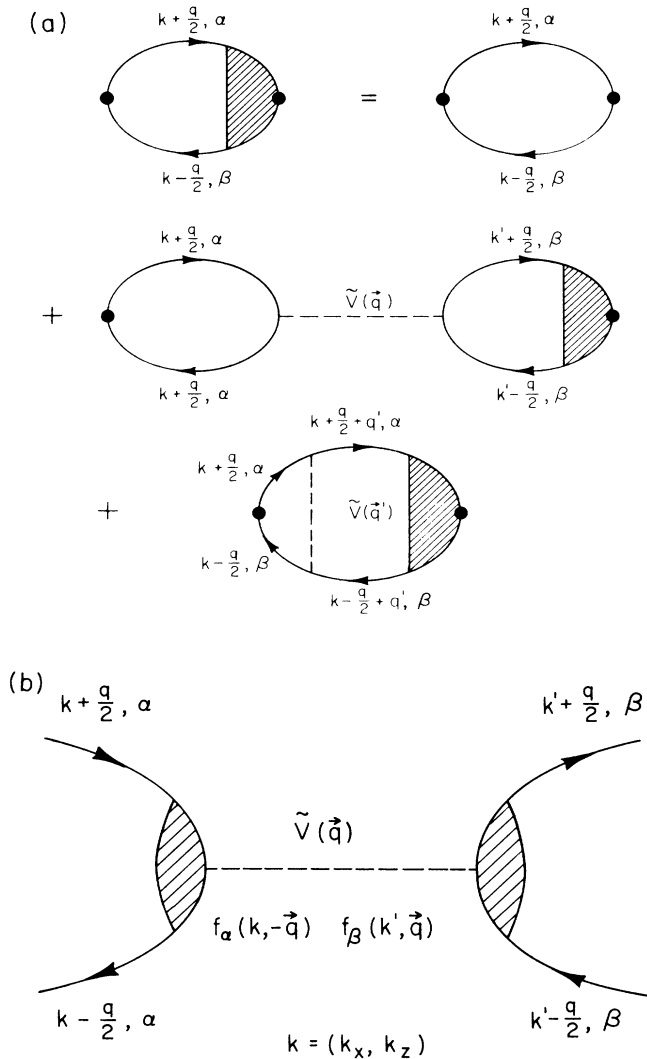
(3.3)

(a)

(b)

$k = (k_x, k_z)$

FIG. 2. (a) Diagrams entering the Hartree-Fock form of the particle-hole correlation function. (b) The renormalization of the bare vertex due to the anisotropy which is ultimately absorbed in particle-hole loops. Latin alphabet letters with arrows denote three-dimensional vectors while those without arrows stand for x and z components only.

where

$$W^{VDW\uparrow(\downarrow)}(q_\perp, q_z = 2k_{\uparrow(\downarrow)}^F)$$

$$= \frac{4\pi e^2 l^2}{\epsilon_0 L^3} \int_0^\infty dx\, e^{-x^2/2} \frac{J_0(lxq_\perp)}{\rho_{\uparrow(\downarrow)}}$$

$$\times \arctan\frac{\rho_{\uparrow(\downarrow)}}{x} .$$

It is easy to see that in both cases the highest transition temperature is obtained for $q_x = q_y = 0$. Both SDW's and VDW's in up- and down-spin bands will be along the direction of the magnetic field. Let us now assume that we can replace the integrands in the exchange interaction by a constant in the momentum space so that the exchange interaction does not depend on $\rho_\uparrow$ and $\rho_\downarrow$; we will justify this later. Then we have $\lambda^{SDW} = 2\kappa/(\rho_\uparrow + \rho_\downarrow)$ and $\lambda^{VDW\uparrow(\downarrow)} = \kappa/\rho_{\uparrow(\downarrow)}$, where κ is some dimensionless parameter (independent of $\rho_\uparrow$ and $\rho_\downarrow$) measuring the interaction strength. Combining this with (3.1) and expressions for E_A^F in the spin- and valley-density wave cases we obtain the following simple relation for transition temperatures:

$$(T_c^{VDW\uparrow} T_c^{VDW\downarrow})^{1/2} = T_c^{SDW} , \qquad (3.4)$$

where $\uparrow(\downarrow)$ denotes an up- (down)-spin band. Equation (3.4) holds for any magnetic field, any number of valleys and arbitrary electron g factor. Thus one of the VDW states always has higher transition temperature than SDW.

To see whether this conclusion remains correct for the exchange interaction appearing in (3.2) and (3.3) we calculate transition temperatures performing the integration over $p_\perp$ numerically. The electronic density n is set to 10^{17} cm^{-3} and the effective mass is taken to be $m = 0.1 m_e$; these numbers we consider to be representative values for semiconductors. The electron gas interaction parameter r_s, which is defined as

$$r_s = \left[\frac{3}{4\pi a_H^3 n} \right]^{1/3} ,$$

a_H being the effective Bohr radius ϵ_0/me^2, where ϵ_0 is the static dielectric constant of the system, is then simply $r_s \cong 25/\epsilon_0$. For most materials of interest $\epsilon_0 > 10$ so that r_s is of order unity. For example, ϵ_0 is 15.8 in Ge and 11.7 in Si. We have actually set $\epsilon_0 = 16$ in our calculation. A more appropriate measure of the interaction strength in strong magnetic field is, however, the ratio of the average potential energy and the kinetic energy in the z direction. We define this new ratio r_s^B as

$$r_s^B = \left[\frac{3}{4\pi} \right]^{1/3} \frac{N_v}{a_H l^2 n} .$$

Note that

$$r_s^B/r_s = (l^2 n^{2/3})^{-1} \sim N_v (lk_F)^{-2/3} .$$

Since in the strong field limit the dimensionless quantity lk_F can become quite small, we see that interactions are strong and that our Hartree-Fock results should only be used as a qualitative guidance.

The results are shown in Fig. 3 as a function of magnetic field, for several values of N_v and electronic g factor. Indeed, the VDW state in the down-spin band has always higher T_c than SDW, indicating that VDW may be the preferred ground state of the system. In fact, Eq. (3.4) is satisfied everywhere to within 5%, providing a posteriori justification for our assumption. As temperature is lowered below $T_c^{\text{VDW}\downarrow}$ we may ask whether the

ground state developing is simply separate VDW's in spin up- and down-bands or some more complicated configuration involving the SDW too. It is easy to show that, in the weak-coupling limit, VDW's in two spin bands are energetically favored over SDW. The condensation energy equals

$$\frac{(T_c^{\text{VDW}\uparrow})^2}{E_\uparrow^F} + \frac{(T_c^{\text{VDW}\downarrow})^2}{E_\downarrow^F}$$

in the former case, while it is $(T_c^{\text{SDW}})^2/(E_\uparrow^F E_\downarrow^F)^{1/2}$ in the latter (the proportionality constant is the same for both cases). Using (3.4) it follows that VDW's have higher condensation energy.
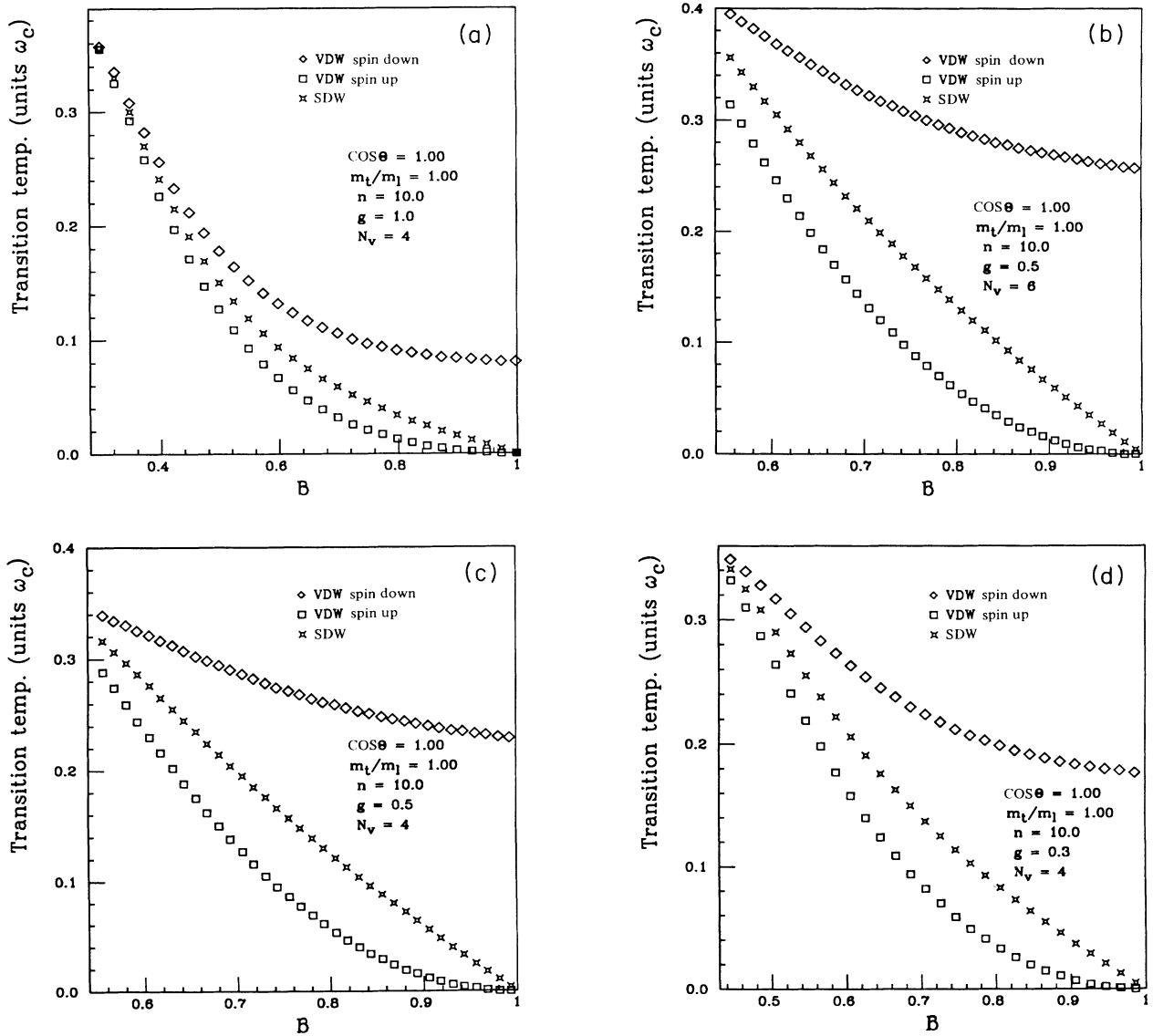

FIG. 3. VDW and SDW transition temperatures measured in units of the cyclotron frequency, for the isotropic case $m_t = m_l$, for various values of the reduced g factor and the valley degeneracy N_v. B_1 is the field at which only the lowest Landau level with both spin states remains occupied, while, for fields larger than B_2, only the spin-down band is populated. Horizontal axis starts at B_1 and ends at B_2 (magnetic field is given in units of B_2). $\bar{g}$ is defined in (2.10), and m_t is set to 0.1 in units of bare electron mass. As explained in the text, the electronic density is 10^{17} cm^{-3}, implying $r_s = 1.56$.

If the coupling is strong the question of the nature of the ground state becomes more complicated since there will be mixing of higher harmonics between VDW and SDW. The mismatch between periods of VDW's in two spin bands may favor SDW and the fully self-consistent solution of the Hartree-Fock equations is necessary to find the true ground state.

IV. ANISOTROPIC CASE

We now consider the effects of valley anisotropy. As long as the magnetic field is in a direction of one of the principal axes of a valley, the effect is simply to properly rescale various quantities with m_t/m_l.

The situation is only slightly more complicated if **B** is in an arbitrary direction as long as the orientations of all valleys are identical. For our model this is achieved if we assume there are only "right" valleys, with $\theta_R = \theta \neq \theta$. Then similar conclusions follow as in the isotropic case: In particular, VDW is the favored state and relation (3.4) is still valid within few percent. The changes are in the values of the "coupling constants" and transition temperatures for various instabilities and the fact that anisotropy changes the basic wave vector at which the instability sets in. For SDW and VDW this wave vector is $q_x = 0$, $q_y = (b_R / a_R) q_z$, where q_z remains as before.

In a typical case, however, the valleys will have different orientations. We investigate this possibility by setting $\theta_R = -\theta_L = \theta$. Let us first assume that there are only two valleys ($N_v = 2$). The SDW state is formed as before containing up- and down-spin bands from each valley with the coupling constant given essentially by (2.6). For a given spin state, we can form two VDW's with different polarization, the one which has an oscillating isospin polarization in the x-y plane, and the one polarized in the z direction of the isospin space; we expect that the most favored direction for the wave vector of the VDW is along the magnetic field, i.e., $q_x = q_y = 0$. Within our model and Fukuyama approximation we find that the VDW polarized along the z direction in the isospin space has somewhat lower transition temperature than the one with polarization in the x-y plane. Therefore, we will discuss only the x-y plane polarized VDW which includes mixing of L and R valleys. The corresponding coupling constant is proportional to W_{LR}. An oscillatory term in (2.7), which is due to anisotropy, reduces W_{LR} relative to $W_{LL(RR)}$ and, if the anisotropy is strong enough, may result in a region of the phase diagram in which SDW is the preferred state. In Fig. 4 we plot transition temperatures of VDW and SDW for several values of θ and m_t/m_l. Again, the density is fixed at 10^{17} cm^{-3}, and the dielectric constant is set to 16, $m_t = 0.1 m_e$. It is natural to define interaction strength parameters r_s and r_s^B in the anisotropic case by replacing the effective mass in a_H by $(m_t^2 m_l)^{1/3}$. In this way a simple formula

$$r_s \cong 16(m_t^2 m_l)^{1/3}$$

can be used to calculate r_s for various situations shown in Fig. 4. From this expression one can easily obtain r_s^B.

Note that, when the anisotropy is strong enough, there is a region of low B where SDW has highest transition temperature. However, VDW ultimately wins as the magnetic field is increased toward B_2. Figure 5 represents the qualitative dependence of dominant instabilities found in our model on anisotropy and g factor. We should mention that the above situation occurs in our model only if $N_v = 2$. As soon as there are more than one left (right) valley a VDW state becomes possible with W_{LL} or W_{RR} as a coupling constant which is again always favored relative to SDW and CDW. From here we conclude that in real systems, when m_t/m_l is not particularly small, VDW is the most probable candidate for the high-field collective state of the electron gas.

We expect that large valley degeneracy in a material like Si will further enhance the VDW instability; a large number of valleys leads to an increase in the number of possible VDW's, some of which are likely to have high transition temperature. It is important to note at this point that in Ge ($g = 1.6$, $g^* \equiv m_t g = 0.09$) the ratio m_t/m_l is as small as 0.057 implying strong valley anisotropy, and consequently the window of stability of SDW can be quite wide, extending over most of the experimentally accessible region of magnetic fields. The possibility of SDW ground state and its properties in Ge has been discussed in Ref. 9.

In Figs. 6(a) and 6(b) we present the results of the calculation of different transition temperatures in our model, for the case of two valleys, with angles $\theta_R = -\theta_L = 0.196\pi$. This situation can be realized in Ge by applying B along the [110] axis and by applying stress along the same axis, so that only [111] and [11$\bar{1}$] valleys remain occupied. The g factor is set to 1.6, its value for Ge, and the transverse and longitudinal effective masses are also taken to represent the band structure of Ge, $m_t = 0.082$ and $m_l = 1.64$ in units of m_e. We find transition temperatures at two different carrier densities, 6×10^{17} cm^{-3} and the density at the metal-insulator transition 2×10^{17} cm^{-3}. These densities correspond to r_s equal to 1.9 and 2.7, respectively. For Figs. 6(c) and 6(d) we have repeated the calculation for the case when all four Ge valleys are occupied (unstressed sample), with magnetic field directly along the [100] axis. Here we consider *only* the case when the direction of VDW is along the magnetic field, which is the situation that can be represented within our model. It is quite possible that other VDW's, with the wave vectors in some other directions, have higher T_c. The results we obtain for these two cases indicate that in Ge the SDW may be stable over significant range of the external magnetic field. We should stress here that the effects of the random impurity potential have been omitted from our model.

V. TRANSPORT PROPERTIES

We expect the transport properties of the SDW and VDW states to be quite remarkable. Due to the formation of the gap at the Fermi energy, the diagonal elements of the conductivity tensor vanish as $T \rightarrow 0$. In the isotropic case, only σ_{xy} and σ_{yx} are different from zero,
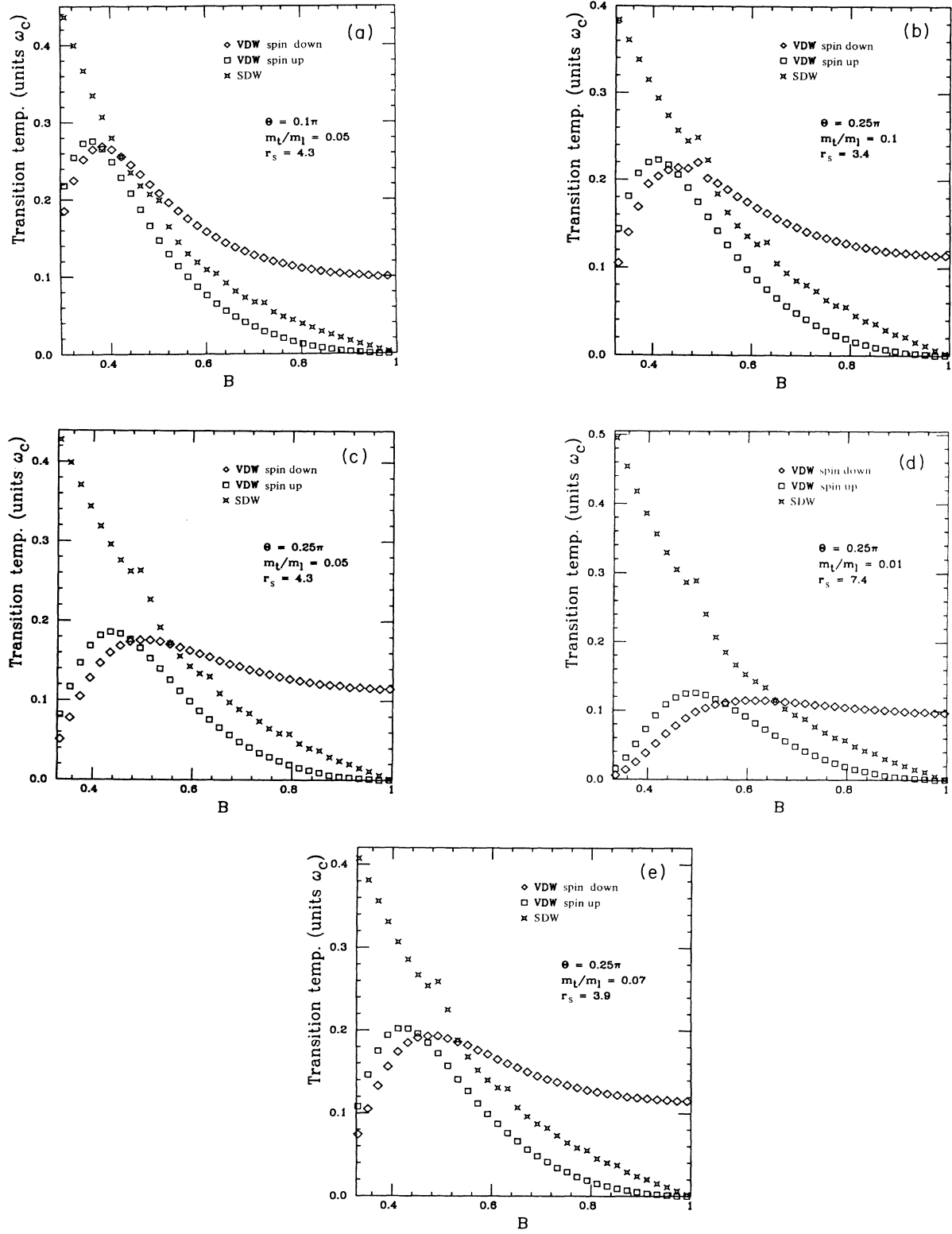
FIG. 4. Transition temperatures as functions of B for various values of θ and m_t/m_l, indicating different degrees of valley anisotropy. The number of valleys is equal to two in all cases, with $\theta_R = -\theta_L$, and $g^* \equiv m_t g$ is fixed to 0.1. That T_c^{SDW} is not smooth at some particular values of B appears to be caused by the systematic error in the routine used to numerically evaluate a two-dimensional integral appearing in λ^{SDW}. We expect that the exact result does not have any sharp structures.

and are given by their *classical* values, i.e., $\sigma_{xy} = -\sigma_{yx} = -nec/B$. Inverting conductivity tensor, we find that the system is an insulator for electric field parallel to $\mathbf{B}(\rho_{\parallel} \to \infty)$, but a perfect conductor in the perpendicular direction $(\rho_{\perp} \to 0)$ as $T \to 0$.

The situation is slightly different for the anisotropic case. Let us first consider a *single* valley rotated with respect to the magnetic field by some angle θ (this corresponds to the case of a single "right" or "left" valley of our model when the axis of rotation is along the x direction). As we have shown in Sec. IV, SDW, or VDW for several such valleys, will not be along the direction of the magnetic field; the angle ϕ_{α} between the field and the direction of the SDW (VDW) is found from $\tan\phi_{\alpha} = b_{\alpha}/a_{\alpha}$. It is easy to show that in this situation, the conductivity tensor has the following form:

$$\sigma = \begin{bmatrix} 0 & (\cos\phi_{\alpha})\sigma_H & -(\sin\phi_{\alpha})\sigma_H \\ -(\cos\phi_{\alpha})\sigma_H & 0 & 0 \\ (\sin\phi_{\alpha})\sigma_H & 0 & 0 \end{bmatrix},$$

where σ_H is the Hall conductivity. Inverting this tensor one finds that *both* $\rho_{\parallel}(=\rho_{zz})$ *and* ρ_{yy} go to infinity when $T \to 0$. ρ_{zy} and ρ_{yz} diverge too. Thus the system is an insulator for electric fields applied along the axis given by the unit vector $(0, \sin\phi_{\alpha}, \cos\phi_{\alpha})$; it remains a perfect conductor in the plane perpendicular to this axis.

When there are several valleys, one must add the conductivity tensors for the various valleys. If there is a "left-right" symmetry, as in our model for the Fermi surface topology with two valleys, $\theta_R = \theta_L$, the σ_{yz} and σ_{zy} components of the conductivity tensor from different valleys cancel out, and once again one finds that the only nonzero components are $\sigma_{xy} = -\sigma_{yx} = -nec/B$.

We may remark that each period of the VDW or

SDW is a layer which contains an integral number of electrons per quantum of magnetic flux, and its transport properties are just what one finds in the quantized Hall effect. If the period of VDW$\uparrow(\downarrow)$ is $\pi/k_{\uparrow(\downarrow)}^F$, then the product of the number of layers per unit length times the quantized Hall conductance per layer $(N_v e^2/h)$ is equal to the classical Hall conductance of the carriers with spin $\uparrow(\downarrow)$. Similar argument holds for SDW. If there is pinning of the VDW or SDW period due to impurities or defects, we might expect the wave vector to deviate slightly from its value in the clean system, and some hysteresis might be expected as the magnetic field is varied at low temperatures. This should lead to a hysteresis in the Hall effect at low temperatures, which may be observable. For further discussion of transport properties see Ref. 9.

VI. CONCLUSIONS

In this paper we have investigated the instabilities of the multivalley electron gas in strong magnetic field. We propose that the ground state of this system, for a wide range of parameters, is the valley-density wave (VDW), as described in the text, but that spin-density wave (SDW) can also occur.

In application of our model to real materials there are several complications that must be kept in mind. Possibly the most serious one concerns the strong impurity scattering due to dopant atoms in degenerate semiconductors. The impurity potential may destroy the collective effects discussed above, resulting in the "magnetic freezeout" of the electron gas. Still, there is a possibility that some of the collective effects will remain, probably in the form of coherent domains of size much larger than the period of VDW (or SDW) or a collection of dislocation lines extending through a sample. The effects of disorder on SDW have been discussed in Ref. 9 and similar conclusions hold for the VDW. We also have to be careful about extending the Hartree-Fock results into the strong-coupling regime of the low-density experimental systems.[13] We expect that, while we cannot rely on Hartree-Fock approximation for quantitative answers, it is still illuminating to use its predictions as a qualitative guidance.[14]
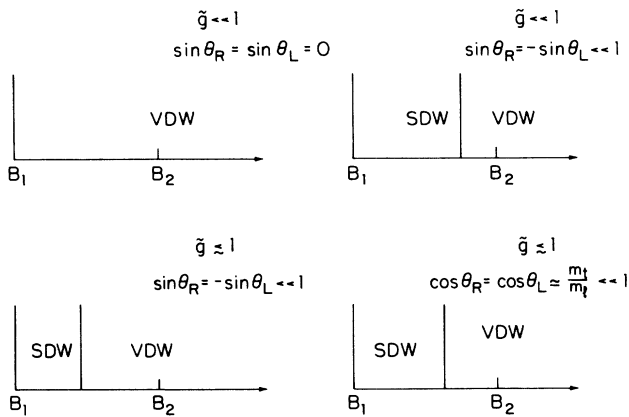
FIG. 5. Qualitative form of the weak-coupling zero temperature phase diagram as a function of the magnetic field, the valley anisotropy, and the effective electronic g factor $\tilde{g}$. The VDW involves combined valley-density waves in up- and down-spin bands up to the magnetic field strength B_2, after which point only the down-spin band remains occupied. The last case corresponds to the extreme anisotropy situation in our model.

APPENDIX A: SINGLE PARTICLE EIGENFUNCTIONS AND EIGENVALUES

In this appendix we calculate single-particle eigenfunctions and energy eigenvalues of an electron with an anisotropic effective-mass tensor in the constant magnetic field directed along the z axis. Let us assume that the effective-mass tensor in its principal frame of reference has the form

$$M_p = \begin{bmatrix} m_t & 0 & 0 \\ 0 & m_t & 0 \\ 0 & 0 & m_l \end{bmatrix} , \qquad (A1)$$

where we assume $m_t < m_l$.

As shown in Fig. 1 the principal axes of M are rotated with respect to the laboratory frame (defined by the direction of magnetic field B) by some angle θ about the x axis. In the laboratory coordinate system the inverse effective-mass tensor (the inverse is needed in Schrödinger equation) is found from

$$M^{-1}=R(\theta)M_p^{-1}R^{-1}(\theta)= \begin{bmatrix} m_t^{-1} & 0 & 0 \\ 0 & m_t^{-1}\cos^2\theta+m_l^{-1}\sin^2\theta & \cos\theta\sin\theta(m_t^{-1}-m_l^{-1}) \\ 0 & \cos\theta\sin\theta(m_t^{-1}-m_l^{-1}) & m_t^{-1}\sin^2\theta+m_l^{-1}\cos^2\theta \end{bmatrix} , \qquad (A2)$$

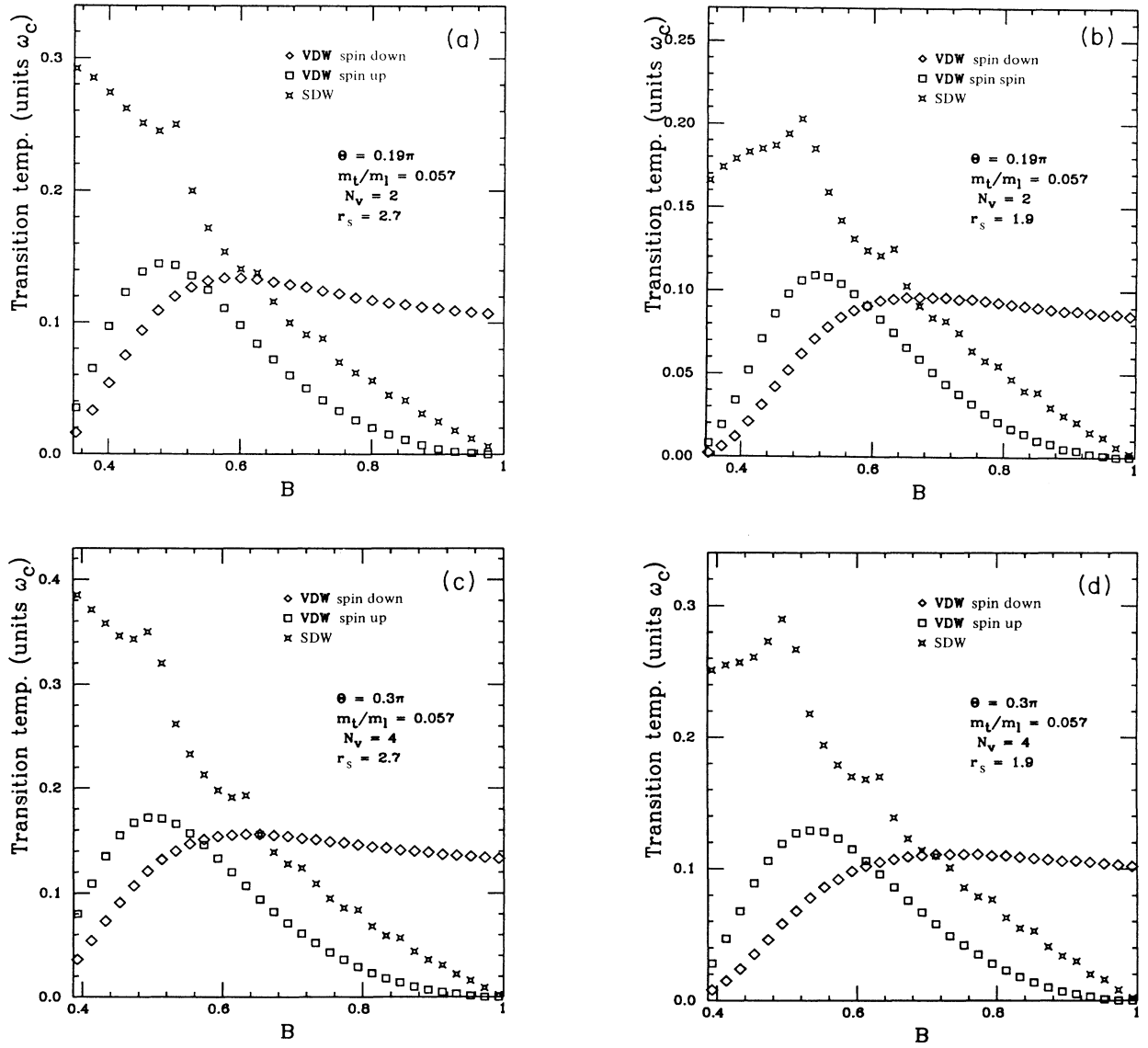with $R(\theta)$ being the corresponding rotation matrix.

FIG. 6. VDW and SDW transition temperatures obtained within our model with the choice of parameters corresponding to Ge. (a) and (b) represent the situations arising when stress is applied along the [110] direction, so that only two valleys are occupied. The magnetic field is also along the [110] axis. The wave vector of VDW is along the magnetic field. (c) and (d) depict cases of an unstressed sample, with all four valleys occupied, and the magnetic field along the [100] axis. The VDW's are restricted to be in the direction of magnetic field. The origin of apparent breaks in T_c^{SDW} is explained in the caption of Fig. 4.

The Schrödinger equation can be written as

$$-\tfrac{1}{2}M_{ij}^{-1}\left[\partial_i-\frac{ie}{c}A_i\right]\left[\partial_j-\frac{ie}{c}A_j\right]\Psi(\mathbf{r})=E\Psi(\mathbf{r})\ , \tag{A3}$$

where $i,j=x,y,z$, $\mathbf{A}$ is the vector potential and summation over repeated indices is implied. We choose to work in the Landau gauge with $\mathbf{A}=(-By,0,0)$. Equation (A3) assumes then the following form:

$$\left[-\frac{1}{2m_t}\left[\partial_x+\frac{ie}{c}By\right]^2-\frac{1}{2}\left[\frac{\cos^2\theta}{m_t}+\frac{\sin^2\theta}{m_l}\right]\partial_y^2-\frac{1}{2}\left[\frac{\sin^2\theta}{m_t}+\frac{\cos^2\theta}{m_l}\right]\partial_z^2\right.$$

$$\left.-(\cos\theta)(\sin\theta)\left[\frac{1}{m_t}-\frac{1}{m_l}\right]\partial_y\partial_z\right]\Psi(\mathbf{r})=E\Psi(\mathbf{r})\ . \tag{A4}$$

In order to find the solution of this equation we first make an *ansatz*

$$\Psi(\mathbf{r})=\exp(ik_x x+ik_z z)\Phi(y)$$

and define $E=\tfrac{1}{2}a'k_z^2+\varepsilon$, where

$$a'\equiv m_t^{-1}\sin^2\theta+m_l^{-1}\cos^2\theta\ .$$

Then we can rewrite (A4) as an equation for $\Phi(y)$:

$$\left[\frac{1}{2m_t}\left[k_x+\frac{eB}{c}y\right]^2-\tfrac{1}{2}a\partial_y^2-ibk_z\partial_y\right]\Phi(y)=\varepsilon\Phi(y)\ , \tag{A5}$$

with

$$a\equiv m_t^{-1}\cos^2\theta+m_l^{-1}\sin^2\theta\ ,$$

and

$$b\equiv\cos\theta\sin\theta(m_t^{-1}-m_l^{-1})\ .$$

Equation (A5) has a familiar form of the linear harmonic oscillator equation with minimum of the potential shifted to $y_0=-ck_z/eB$. However, unlike the standard case, there is additional term coupling k_z and ∂_y. This term simply introduces translation in the *momentum* space, i.e., $p_y\to p_y+(b/a)k_z$. Therefore, we can write the solution as

$$\Phi(y+l^2k_x)=\int\frac{dp_y}{2\pi}e^{ip_y(y+l^2k_x)}\Upsilon\left[p_y-\frac{b}{a}k_z\right]\ , \tag{A6}$$

where $\Upsilon[p-(b/a)k_z]$ is the momentum space eigenfunction of the Schrödinger equation without the term coupling ∂_y and k_z. These eigenfunctions are just the standard solution of the Schrödinger equation for electron in constant magnetic field and after some straightforward manipulations we can finally write the eigenfunctions and eigenvalues in the form given in the text.

APPENDIX B: THE SINGLE-PARTICLE OPERATORS $A(\mathbf{q},t)$

In this appendix we give an explicit second-quantization form of various single-particle operators that appear in the response functions we will be considering. The particle-density operator can be written as

$$\rho(\mathbf{q},t)=\sum_{k_x,k_z}\sum_{\alpha,s}c^\dagger_{k_x-1/2q_x,k_z-1/2q_z,\alpha s}(t)c_{k_x+1/2q_x,k_z+1/2q_z,\alpha s}(t)$$

$$\times\exp[-iu_\alpha l^2(k_zq_x+k_xq_z)+il^2(q_y+u_\alpha q_z)k_x]\exp\left[-\frac{l^4}{4l_\alpha^2}q_x^2-\frac{l_\alpha^2}{4}(q_y+u_\alpha q_z)^2\right]\ , \tag{B1}$$

where $c^\dagger_{k_x k_z,\alpha s}(t)$ is the electron creation operator in the Heisenberg representation, and $u_\alpha\equiv b_\alpha/a_\alpha$.

The spin-density operator we can write as

$$\sigma(\mathbf{q},t)=\sum_{k_x,k_z}\sum_\alpha\sum_{s_1,s_2}c^\dagger_{k_x-1/2q_x,k_z-1/2q_z,\alpha s_1}(t)c_{k_x+1/2q_x,k_z+1/2q_z,\alpha s_2}(t)(2\mathbf{S})_{s_1 s_2}$$

$$\times\exp[-iu_\alpha l^2(k_zq_x+k_xq_z)+il^2(q_y+u_\alpha q_z)k_x]\exp\left[-\frac{l^4}{4l_\alpha^2}q_x^2-\frac{l_\alpha^2}{4}(q_y+u_\alpha q_z)^2\right]\ , \tag{B2}$$

where $\mathbf{S}$ is the spin angular momentum operator. In the spin space its components are just the ordinary Pauli matrices, i.e., $2\mathbf{S}=(\gamma_x,\gamma_y,\gamma_z)$ where:

$$\gamma_x=\begin{bmatrix}0&1\\1&0\end{bmatrix},\quad\gamma_y=\begin{bmatrix}0&-i\\i&0\end{bmatrix},\quad\gamma_z=\begin{bmatrix}1&0\\0&-1\end{bmatrix}\ .$$

The "valley-density" operator can be defined for the case when there are "right" and "left" valleys using the analogy with the spin degree of freedom

$$\tau(\mathbf{q},t) = \sum_{k_x,k_z} \sum_{\alpha,\beta} \sum_s c^\dagger_{k_x,k_z,\alpha s}(t) c_{k_x+q_x,k_z+q_z,\beta s}(t)(2\mathbf{I})_{\alpha\beta}$$

$$\times \exp[i(u_\alpha - u_\beta)l^2 k_x k_z - iu_\beta l^2(k_z q_x + k_x q_z) - iu_\beta q_x q_z]$$

$$\times \exp\left[-\frac{l^4}{4\tilde{l}^2}q_x^2 - \frac{\tilde{l}^2}{4}[q_y + u_\beta q_z - (u_\alpha - u_\beta)k_z]^2 \right.$$

$$\left. + il^2[q_y + u_\beta q_z - (u_\alpha - u_\beta)k_z](k_x + \tfrac{1}{2}q_x) \right] , \qquad \text{(B3)}$$

where we have used the fact that in our model $l_R = l_L \equiv \tilde{l}$ and $\mathbf{I}$ is the "isospin" operator. The components of $\mathbf{I}$ are Pauli matrices in the *isospin* space: $2\mathbf{I} = (\gamma_x, \gamma_y, \gamma_z)$.

The matrix elements $\langle \alpha s_1 | \Theta_A | \beta s_2 \rangle$ are then given explicitly as $\delta_{\alpha\beta}\delta_{s_1 s_2}$ for $A = \rho$ ($\Theta_A = 1$), $\delta_{\alpha\beta}\gamma_{s_1 s_2}$ for $A = \sigma$ ($\Theta_A = 2\mathbf{S}$), and $\gamma_{\alpha\beta}\delta_{s_1 s_2}$ for $A = \tau$ ($\Theta_A = 2\mathbf{I}$). We note that the "isospin" operators commute with the Hamiltonian of our model in the case where the two valleys have identical orientation.

In general, if there is a nonzero expectation value $\langle \tau_x(\mathbf{q}) \rangle$, or $\langle \tau_y(\mathbf{q}) \rangle$, then there are nonzero expectation values of the form $\langle c^\dagger_{k_x,k_z,\alpha s} c_{k_x+q_x,k_z+q_z,\beta s} \rangle$ for $\alpha \neq \beta$. This may lead in turn to nonzero expectation values of the electron density or of the transverse electron current, at a wave vector $\mathbf{Q} + \mathbf{G} + \mathbf{q}$, where $\mathbf{Q}$ is the difference between the positions of valleys β and α in the Brillouin zone of the crystal, and $\mathbf{G}$ is an arbitrary reciprocal lattice vector. (The appearance of a modulated electron current may be alternatively described as a type of orbital antiferromagnetism.) Similar modulations may also occur in the case where $\langle \tau_z \rangle \neq 0$. The precise forms of the possible modulations will depend on the symmetries of the system in question.

APPENDIX C: EVALUATION OF MATRIX ELEMENTS

The interaction term in Hamiltonian (2.1) can be written as (since the interaction is spin independent we can drop spin indices in what follows):

$$H_{\text{int}} = \frac{1}{2} \sum_{\bar{k}_1,\bar{k}_2,\bar{k}_3,\bar{k}_4} c^\dagger_{\bar{k}_1\alpha} c^\dagger_{\bar{k}_2\beta} c_{\bar{k}_3\beta} c_{\bar{k}_4\alpha} \Gamma^{\alpha\beta}(\bar{k}_1,\bar{k}_2,\bar{k}_3,\bar{k}_4) , \qquad \text{(C1)}$$

where $\bar{k} \equiv (k_x, k_z)$ and

$$\Gamma^{\alpha\beta}(\bar{k}_1,\bar{k}_2,\bar{k}_3,\bar{k}_4) = \sum_q \frac{V(\mathbf{q})}{L^3} \int d^3 r_1 \int d^3 r_2 e^{i\mathbf{q}\cdot(\mathbf{r}_1-\mathbf{r}_2)} \Psi_{\bar{k}_1\alpha}(\mathbf{r}_1)^* \Psi_{\bar{k}_2\beta}(\mathbf{r}_2)^* \Psi_{\bar{k}_3\beta}(\mathbf{r}_2) \Psi_{\bar{k}_4\alpha}(\mathbf{r}_1) , \qquad \text{(C2)}$$

where $\Psi_{\bar{k}\alpha}(\mathbf{r})$ are the electron eigenfunctions defined in the text; we here consider only the electrons in the lowest Landau level.

To evaluate (C2) we first perform the integration over z and x coordinates. If we write $\Psi_{\bar{k}\alpha}(\mathbf{r})$ as $1/L \exp(ik_z z + ik_x x)\varphi_{k\alpha}(y)$ the result of the integration is

$$\Gamma^{\alpha\beta}(\bar{k}_1,\bar{k}_2,\bar{k}_3,\bar{k}_4) = \sum_q \frac{V(\mathbf{q})}{L^3} \delta_{\bar{k}_1,\bar{k}_4+q} \delta_{\bar{k}_2,\bar{k}_3-q} \gamma_\alpha(\bar{k}_4,\mathbf{q}) \gamma_\beta(\bar{k}_3, -\mathbf{q}) ,$$

with $\mathbf{q} \equiv (q_x, q_z)$ and

$$\gamma_\alpha(\bar{k}_4,\mathbf{q}) = \int dy\, e^{iq_y y} \varphi^*_{\bar{k}_4+q\alpha}(y) \varphi_{\bar{k}_4\alpha}(y) . \qquad \text{(C3)}$$

The function $\gamma_\alpha(\bar{k}_4,\mathbf{q})$ is found by integrating over y using the explicit form for $\varphi_{\bar{k}_4\alpha}(y)$ given in the text. After some algebra we find

$$\gamma_\alpha(\bar{k},\mathbf{q}) = \exp\left[-\frac{l^4}{4l_\alpha^2}q_x^2 - \frac{l_\alpha^2}{4}q_y^2 + il^2 k_x q_y + \frac{i}{2}l^2 q_x q_y \right] \exp\left[-i\frac{b_\alpha}{2a_\alpha}l^2 q_x q_z - i\frac{b_\alpha}{a_\alpha}l^2 k_z q_x - \frac{l_\alpha^2 b_\alpha}{2a_\alpha}q_y q_z - \frac{l_\alpha^2 b_\alpha^2}{4a_\alpha^2}q_z^2 \right] , \qquad \text{(C4)}$$

where a_α and b_α have been defined previously. Going back to (C1) and changing $\bar{k}_4 \to \bar{k}_4 - \tfrac{1}{2}\mathbf{q}$ and $\bar{k}_3 \to \bar{k}_3 + \tfrac{1}{2}\mathbf{q}$ we obtain the final form for the interaction term in the Hamiltonian

$$H_{\text{int}} = \sum_{q,\alpha,\beta} \frac{1}{2L^3} \tilde{V}(\mathbf{q}) \sum_{\bar{k}_3,\bar{k}_4} e^{-il^2(k_{4_x}-k_{3_x})q_y} f_\alpha(\bar{k}_4,\mathbf{q}) f_\beta(\bar{k}_3,-\mathbf{q}) c^\dagger_{\bar{k}_4+1/2q,\alpha} c^\dagger_{\bar{k}_3-1/2q,\beta} c_{\bar{k}_3+1/2q,\beta} c_{\bar{k}_4-1/2q,\alpha} \ , \tag{C5}$$

where

$$\tilde{V}_{\alpha\beta}(\mathbf{q}) = V(\mathbf{q})\exp\left\{ -\left[\frac{l^4}{4l_\alpha^2}+\frac{l^4}{4l_\beta^2}\right]q_x^2 - \left[\frac{l_\alpha^2}{4}+\frac{l_\beta^2}{4}\right]q_y^2 \right\}$$

and

$$f_\alpha(\mathbf{k},\mathbf{q})=\exp\left[-i\frac{b_\alpha}{a_\alpha}l^2 k_z q_x + \frac{l_\alpha^2 b_\alpha}{2a_\alpha}q_y q_z - \frac{l_\alpha^2 b_\alpha^2}{4a_\alpha^2}q_z^2 \right] .$$

*Present address: Theoretical Division, MS B262, Los Alamos National Laboratory, Los Alamos, NM 87545.

[1]V. Celli and N. D. Mermin, Phys. Rev. A **140**, 839 (1965).

[2]W. G. Kleppmann and R. J. Elliot, J. Phys. C **8**, 2729 (1975).

[3]A. H. MacDonald and G. W. Bryant (unpublished).

[4]D. Yoshioka and H. Fukuyama, J. Phys. Soc. Jpn. **50**, 725 (1981).

[5]R. Gerhardts and P. Schlottmann, Z. Phys. B **34**, 349 (1979).

[6]H. Schulz and H. Keiter, J. Low Temp. Phys. **11**, 181 (1973).

[7]H. Fukuyama, Solid State Commun. **26**, 783 (1978).

[8]Y. Iye, L. E. McNeil, and G. Dresselhaus, Phys. Rev. B **30**, 7009 (1984).

[9]For example, see B. I. Halperin, to appear in *Condensed Matter Theories*, Proceedings of the Argonne International Workshop on Many-Body Physics, edited by P. Vashista *et al.* (Plenum, New York, 1986), and references therein.

[10]M. Rasolt, B. I. Halperin, and David Vanderbilt, Phys. Rev. Lett. **57**, 126 (1986).

[11]We use notation and conventions of C. Kallin and B. I. Halperin, Phys. Rev. B **30**, 5655 (1984).

[12]Alternatively, we can set $\theta_L = \theta_R = 0$ and still keep $m_t \neq m_l$.

[13]In this context, having to deal both with the strong electron-electron coupling and strong disorder, it may be worthwhile the exploit the number of valleys as an expansion parameter. A meaningful $1/N_v$ expansion can be formulated within our model and both the electron-electron interaction and disorder can be treated within its rigorous scheme: Z. Tešanović and M. Rasolt (unpublished).

[14]Here we should mention that, as magnetic field increases, the corresponding reduction in the kinetic energy in the z direction may lead to a formation of the valley-polarized state: M. Rasolt, Phys. Rev. Lett. **55**, 433 (1985).